To appear in *Molecular Physics*
Vol. 00, No. 00, Month 200x, 1–20

RESEARCH ARTICLE

Molecular Properties in the Tamm–Dancoff Approximation: Indirect Nuclear Spin–Spin Coupling Constants

Chi Y. Cheng[a], Matthew S. Ryley[a], Michael J. G. Peach[b], David J. Tozer[c], Trygve Helgaker[d], Andrew M. Teale[a,d,*]

[a] School of Chemistry, University of Nottingham, University Park, Nottingham, UK, NG7 2RD

[b] Department of Chemistry, Lancaster University, Lancaster, UK, LA1 4YB

[c] Department of Chemistry, Durham University, South Road, Durham, UK, DH1 3LE

[d] Department of Chemistry, Centre for Theoretical and Computational Chemistry, University of Oslo, P.O. Box 1033 Blindern, N-0315 Oslo, Norway

(*Received 00 Month 200x; final version received 00 Month 200x*)

The Tamm–Dancoff approximation (TDA) can be applied to the computation of excitation energies using time-dependent Hartree–Fock (TD-HF) and time-dependent density-functional theory (TD-DFT). In addition to simplifying the resulting response equations, the TDA has been shown to significantly improve the calculation of triplet excitation energies in these theories, largely overcoming issues associated with triplet instabilities of the underlying reference wave functions. Here, we examine the application of the TDA to the calculation of another response property involving triplet perturbations, namely the indirect nuclear spin–spin coupling constant. Particular attention is paid to the accuracy of the triplet spin–dipole and Fermi-contact components. The application of the TDA in HF calculations leads to vastly improved results. For DFT calculations, the TDA delivers improved stability with respect to geometrical variations but does not deliver higher accuracy close to equilibrium geometries. These observations are rationalized in terms of the ground- and excited-state potential energy surfaces and, in particular, the severity of the triplet instabilities associated with each method. A notable feature of the DFT results within the TDA is their similarity across a wide range of different functionals. The uniformity of the TDA results suggests that some conventional evaluations may exploit error cancellations between approximations in the functional forms and those arising from triplet instabilities. The importance of an accurate treatment of correlation for evaluating spin–spin coupling constants is highlighted by this comparison.

Keywords: nuclear magnetic resonance; spin–spin coupling constants; Hartree–Fock theory; density–functional theory; coupled-cluster theory

1. Introduction

The reliable calculation of triplet response properties remains a challenging task for single-reference approaches such as Hartree–Fock (HF) theory and Kohn–Sham (KS) density-functional theory (DFT). Issues associated with HF triplet instabilities have been widely discussed in the literature [1–4]. In the context of DFT, the issues [5] are further complicated by the observation that the stability of calculated triplet properties can be dependent on the choice of exchange–correlation functional [6, 7].

*Corresponding author: andrew.teale@nottingham.ac.uk

ISSN: 0040-5167 print/ISSN 1754-2278 online

DOI: 10.1080/0040516YYxxxxxxxx
http://www.informaworld.com

For the calculation of triplet excitation energies, the Tamm–Dancoff approximation [8, 9] (TDA) has been applied using time-dependent Hartree–Fock (TD-HF) and time-dependent density-functional theory (TD-DFT). This simple approach not only leads to computationally more tractable response equations but has also been shown to significantly improve the calculation of triplet excitation energies in these theories, largely overcoming issues associated with triplet instabilities [2, 10–16].

In this work, we consider the application of the TDA to the calculation of another response property involving triplet perturbations, namely the indirect nuclear spin–spin coupling constant. Computationally, the accurate calculation of this quantity is challenging because it is composed of a range of different components, including the triplet spin–dipole and Fermi-contact components. We assess the performance of the TDA at the HF and KS-DFT levels by comparing the results for the isotropic spin–spin coupling constants and their components with those from the higher-level second-order polarization propagator approximation (SOPPA) and coupled-cluster (CC) theories.

We commence in Section 2 by outlining the theory necessary for the computation of spin–spin couplings at the HF and DFT levels, as well as how the TDA may be introduced in these calculations. In Section 4, we first analyze the quality of the approximation over a broad range of coupling constants in small molecular systems close to their equilibrium geometries. We then examine the stability of the calculations in more detail for a representative molecule as a function of geometry, highlighting the important role of the reference state in the calculations. Finally, in Section 5, we present some concluding remarks and directions for future work.

2. Theory

The theory for the evaluation of spin–spin coupling constants is reviewed in detail in Ref. [17]. Here, we give a brief overview of the relevant theory to establish notation and show how the TDA may be introduced.

2.1. *Sum-Over-States Formulation*

Although computationally cumbersome, the sum-over-states approach leads to the conceptually simplest computational evaluation of the reduced spin–spin coupling tensor. This tensor, $\mathbf{K}_{KL}$, is given by the sum-over-states expression presented by Ramsey in 1953 [18]. This formula serves to illustrate the main contributions into which the spin–spin couplings can be decomposed and the different roles of singlet and triplet excited states,

$$\begin{aligned}\mathbf{K}_{KL} = \left\langle 0 \left| \mathbf{h}_{KL}^{\mathrm{DSO}} \right| 0 \right\rangle &- 2 \sum_{n_S \neq 0} \frac{\left\langle 0 \left| \mathbf{h}_{K}^{\mathrm{PSO}} \right| n_S \right\rangle \left\langle n_S \left| (\mathbf{h}_{L}^{\mathrm{PSO}})^{\mathrm{T}} \right| 0 \right\rangle}{E_{n_S} - E_0} \\ &- 2 \sum_{n_T} \frac{\left\langle 0 \left| \mathbf{h}_{K}^{\mathrm{FC}} + \mathbf{h}_{K}^{\mathrm{SD}} \right| n_T \right\rangle \left\langle n_T \left| (\mathbf{h}_{L}^{\mathrm{FC}})^{\mathrm{T}} + (\mathbf{h}_{L}^{\mathrm{SD}})^{\mathrm{T}} \right| 0 \right\rangle}{E_{n_T} - E_0}. \end{aligned} \tag{1}$$

Here the diamagnetic spin–orbit (DSO), paramagnetic spin–orbit (PSO), Fermi-contact (FC) and spin–dipole (SD) operators in atomic units are

$$\mathbf{h}_{KL}^{\mathrm{DSO}} = \alpha^4 \sum_i \frac{\mathbf{r}_{iK}^{\mathrm{T}} \mathbf{r}_{iL} \mathbf{I}_3 - \mathbf{r}_{iK} \mathbf{r}_{iL}^{\mathrm{T}}}{r_{iK}^3 r_{iL}^3}, \tag{2}$$

$$\mathbf{h}_K^{\mathrm{PSO}} = -\mathrm{i}\alpha^2 \sum_i \frac{\mathbf{r}_{iK} \times \nabla_i}{r_{ik}^3}, \tag{3}$$

$$\mathbf{h}_K^{\mathrm{FC}} = \frac{8\pi\alpha^2}{3} \sum_i \delta(\mathbf{r}_{iK})\mathbf{s}_i, \tag{4}$$

$$\mathbf{h}_K^{\mathrm{SD}} = \alpha^2 \sum_i \frac{3\mathbf{r}_{iK}^{\mathrm{T}}\mathbf{s}_i\mathbf{r}_{iK} - r_{iK}^2\mathbf{s}_i}{r_{iK}^5}, \tag{5}$$

where α is the fine-structure constant, $\mathbf{r}_{iK}$ is the position of electron i relative to nucleus K, $\mathbf{I}_3$ is the three-by-three unit matrix, $\delta(\mathbf{r}_{iK})$ is the Dirac delta function, and $\mathbf{s}_i$ is the spin of electron i. The summations run over all excited singlet states $|n_S\rangle$ with energy E_{n_S} and all triplet states $|n_T\rangle$ with energy E_{n_T}. A few key points can be noted from this expression. First, all of the contributions are local to the nuclei. The DSO, PSO and SD terms involve denominators in the electron–nuclear distances. The FC term is extremely local in that its contributions are only from electrons at the nuclei. Second, although all terms contribute, in most cases—in particular, for one-bond coupling constants—it is the terms involving the FC operator that dominate (note the pre-factor above). Finally, from Eq. (1), we can see that the FC and SD components are of triplet type, whereas the PSO term is of singlet type.

From a computational point of view, the reduced coupling tensor $\mathbf{K}_{KL}$ is dependent purely on the electronic structure in the Born–Oppenheimer approximation. Its evaluation requires only expectation values involving ground- and excited-state electronic wave functions and their associated excitation energies. This reduced quantity is related to the coupling tensor

$$\mathbf{J}_{KL} = h\frac{\gamma_K}{2\pi}\frac{\gamma_L}{2\pi}\mathbf{K}_{KL}, \tag{6}$$

where γ_K is the gyromagnetic ratio of nucleus K and h is the Planck constant. Throughout this work, we focus on the isotropic spin–spin coupling constant (and the corresponding DSO, PSO, FC and SD components), defined as

$$J_{KL} = \frac{1}{3}\mathrm{Tr}\mathbf{J}_{KL}. \tag{7}$$

This quantity can be observed experimentally for freely tumbling molecules in the liquid or gas phases using high-resolution nuclear magnetic resonance spectroscopy.

2.2. *Response-Theory Formulation*

A more computationally tractable (but formally equivalent) approach arises from the use of linear response theory to calculate spin–spin coupling constants. The spin–spin coupling tensor for nuclei K and L is given by

$$\mathbf{K}_{KL} = \frac{\partial^2 E}{\partial\mathbf{m}_K\partial\mathbf{m}_L} + \frac{\partial^2 E}{\partial\mathbf{m}_K\partial\kappa}\frac{\partial\kappa}{\partial\mathbf{m}_L}. \tag{8}$$

Here, the linear response of the wave function $\partial\kappa/\partial\mathbf{m}_L$ can be obtained from the linear response equations

$$\frac{\partial^2 E}{\partial\kappa\partial\kappa}\frac{\partial\kappa}{\partial\mathbf{m}_L} = -\frac{\partial^2 E}{\partial\kappa\partial\mathbf{m}_L}, \tag{9}$$

where κ are the wave function parameters. The response equations may be expressed in the compact form,

$$\mathbf{G}\lambda_L = -\mathbf{R}_L. \tag{10}$$

For single-reference approaches such as KS-DFT and HF theory, the right-hand side may be expressed in terms of occupied–virtual orbital rotations κ_{ai} as

$$\mathbf{R}_{L,ai} = \frac{\partial^2 E}{\partial\kappa_{ai}\partial\mathbf{m}_L}. \tag{11}$$

The linear response equations can be separated into components for the PSO, SD and FC contributions in the manner

$$\sum_{bj} {}^{\mathrm{II}}\mathbf{G}^{ss}_{ai,bj}\lambda^{\mathrm{PSO}}_{L,bj} = -\mathbf{R}^{\mathrm{PSO}}_{L,ai}, \tag{12}$$

$$\sum_{bj} {}^{\mathrm{RR}}\mathbf{G}^{tt}_{ai,bj}\lambda^{\mathrm{SD}}_{L,bj} = -\mathbf{R}^{\mathrm{SD}}_{L,ai}, \tag{13}$$

$$\sum_{bj} {}^{\mathrm{RR}}\mathbf{G}^{tt}_{ai,bj}\lambda^{\mathrm{FC}}_{L,bj} = -R^{\mathrm{FC}}_{L,ai}, \tag{14}$$

where

$$\mathbf{R}^{\mathrm{PSO}}_{L,ai} = 2\alpha^2 \int \varphi_a(\mathbf{r}) r_L^{-3}\mathbf{r}_L \times \nabla\varphi_i(\mathbf{r})\mathrm{d}\mathbf{r}, \tag{15}$$

$$\mathbf{R}^{\mathrm{SD}}_{L,ai} = \alpha^2 \int \varphi_a(\mathbf{r}) r_L^{-5}(3\mathbf{r}_L\mathbf{r}_L^{\mathrm{T}} - r_L^2\mathbf{I}_3)\varphi_i(\mathbf{r})\mathrm{d}\mathbf{r}, \tag{16}$$

$$R^{\mathrm{FC}}_{L,ai} = \frac{8\pi\alpha^2}{3}\varphi_a(\mathbf{r}_L)\varphi_i(\mathbf{r}_L). \tag{17}$$

The response equations include the electronic Hessians for imaginary (I) singlet (s) rotations ${}^{\mathrm{II}}\mathbf{G}^{ss}_{ai,bj}$ and real (R) triplet (t) rotations ${}^{\mathrm{RR}}\mathbf{G}^{tt}_{ai,bj}$. The corresponding contributions to the spin–spin coupling tensor are calculated as

$$\mathbf{K}^{\mathrm{PSO}}_{KL} = \sum_{ai} \lambda^{\mathrm{PSO}}_{K,ai}(\mathbf{R}^{\mathrm{PSO}}_{L,ai})^{\mathrm{T}}, \tag{18}$$

$$\mathbf{K}^{\mathrm{SD}}_{KL} = \sum_{ai} \lambda^{\mathrm{SD}}_{K,ai}(\mathbf{R}^{\mathrm{SD}}_{L,ai})^{\mathrm{T}}, \tag{19}$$

$$\mathbf{K}^{\mathrm{FC}}_{KL} = \mathbf{I}_3 \sum_{ai} i\lambda^{\mathrm{FC}}_{K,ai}R^{\mathrm{FC}}_{L,ai}, \tag{20}$$

$$\mathbf{K}^{\mathrm{FC/SD}}_{KL} = \sum_{ai} \lambda^{\mathrm{SD}}_{K,ai}R^{\mathrm{FC}}_{L,ai} + \sum_{ai} \lambda^{\mathrm{FC}}_{K,ai}\mathbf{R}^{\mathrm{SD}}_{L,ai} \tag{21}$$

along with the DSO contribution, which is given by the expectation value

$$\mathbf{K}_{KL}^{\mathrm{DSO}} = 2\alpha^4 \sum_i \int \varphi_i(\mathbf{r}) \frac{\mathbf{r}_K^{\mathrm{T}}\mathbf{r}_L\mathbf{I}_3 - \mathbf{r}_K\mathbf{r}_L^{\mathrm{T}}}{r_K^3 r_L^3} \varphi_i(\mathbf{r}_i)\mathrm{d}\mathbf{r}_i. \tag{22}$$

2.3. *TDA for Spin–Spin Coupling Constants*

The connection between the limited accuracy of DFT for spin–spin couplings and the triplet instability that affects the calculation of triplet excitation energies was recently explored by Lutnæs *et al.* [7]. The triplet instability causes the triplet excitations to be too low in general and strongly dependent on the molecular geometry. Lutnæs *et al.* observed that density functionals that suffer least from triplet instabilities offer a more stable or robust description of spin–spin couplings, whilst those that offer higher accuracy tend to be more strongly afflicted and require practical calculations at or very close to the molecular equilibrium geometry. Often this is because the functionals include a fraction of the HF exchange contribution. In the context of HF theory, the triplet instability issues associated with evaluating spin–spin coupling constants dominate to the extent that practical results at this level cannot be used [19, 20]. It has long been known that the TDA [8, 9] can be applied in the calculation of excitation energies and gives results that are essentially free of errors associated with the triplet instability [10, 11]. However, to the best of our knowledge, this approximation has not been applied to other molecular properties involving triplet perturbations.

The orbital-rotation Hessians for general singlet or triplet rotations can be expressed as

$$^{\mathrm{II}}\mathbf{G}^{uu} = (^{u}\mathbf{A} - {}^{u}\mathbf{B}), \tag{23}$$

$$^{\mathrm{RR}}\mathbf{G}^{uu} = (^{u}\mathbf{A} + {}^{u}\mathbf{B}), \tag{24}$$

where

$$(^{s}A - {}^{s}B)_{ij,ab} = \delta_{ij}\delta_{ab}(\varepsilon_a - \varepsilon_i) - \gamma g_{ijab} + \gamma g_{ajbi} - (ij|f_{\mathrm{xc}}|ab) + (aj|f_{\mathrm{xc}}|bi), \tag{25}$$

$$(^{s}A + {}^{s}B)_{ij,ab} = \delta_{ij}\delta_{ab}(\varepsilon_a - \varepsilon_i) + 4g_{iajb} - \gamma g_{ijab} - \gamma g_{ajbi} - (ij|f_{\mathrm{xc}}|ab) + (aj|f_{\mathrm{xc}}|bi), \tag{26}$$

$$(^{t}A - {}^{t}B)_{ij,ab} = \delta_{ij}\delta_{ab}(\varepsilon_a - \varepsilon_i) - \gamma g_{ijba} + \gamma g_{ajbi} - (ij|f_{\mathrm{xc}}|ab) + (aj|f_{\mathrm{xc}}|bi), \tag{27}$$

$$(^{t}A + {}^{t}B)_{ij,ab} = \delta_{ij}\delta_{ab}(\varepsilon_a - \varepsilon_i) - \gamma g_{ijba} - \gamma g_{ajbi} - (ij|f_{\mathrm{xc}}|ab) - (aj|f_{\mathrm{xc}}|bi). \tag{28}$$

Here ε_p are the orbital energies, γ is the amount of Hartree–Fock exchange, f_{xc} is the exchange–correlation kernel and g_{pqrs} represent standard electron repulsion integrals. In the case of range-separated exchange–correlation functionals, such as CAM-B3LYP used in this work, the above equations may be modified easily by replacing the γ-scaled repulsion integrals with their long-range counterparts. In the sum-over-states formulation of Section 2.1, these orbital-rotation Hessians can be used to determine the excitation energies via the TDHF or TDDFT equations. In the response formulation of Section 2.2, these orbital-rotation Hessians enter directly as $^{\mathrm{II}}\mathbf{G}^{uu}$ and $^{\mathrm{RR}}\mathbf{G}^{uu}$. The sum-over-states and response formulations are, of course, equivalent. However, whereas the sum-over-states formulation gives a clear intuitive picture of the relevance of excitation energies in the computation of spin–spin couplings, the response formulation is more computationally efficient,

avoiding the need for the explicit calculation of all excitation energies.

The TDA is most frequently applied in the calculation of excitation energies. It is defined by setting

$$^{u}\mathbf{B} = \mathbf{0}. \tag{29}$$

In the sum-over-states formulation, this corresponds to applying the TDA approximation in the calculation of excitation energies via the TDHF or TDDFT equations entering the denominators of Eq. (1). Equivalently, in the response formulation, the TDA corresponds to

$$^{\mathrm{II}}\mathbf{G}^{uu} = {}^{\mathrm{RR}}\mathbf{G}^{uu} = {}^{u}\mathbf{A}. \tag{30}$$

In this work, we investigate the effect that the application of the TDA has on the calculation of spin–spin coupling constants.

Lutnæs *et al.* [7] have shown the close connection between the quality of conventional evaluations in KS-DFT and the onset of triplet instabilities for a variety of functionals. These issues afflict the SD and FC contributions in particular due to their triplet symmetry. Since the latter often accounts for the bulk of the spin–spin coupling values, the application of the TDA to these quantities is of particular interest.

3. Computational Details

We have implemented the TDA in the flexible response module [21–23] of the DALTON quantum chemistry program [24, 25]. This implementation allows for the calculation of a range of properties within the TDA. All HF and DFT calculations are carried out in a spin-restricted formalism. We consider the application of the TDA uniformly in the calculations (i.e., also to the response evaluation of the singlet PSO term) and quantify its influence in HF and DFT calculations. To benchmark our results, we use SOPPA(CC2) and SOPPA(CCSD) coupling constants [26–29] calculated with the DALTON program, and CCSD constants, excluding orbital relaxation contributions [30], from the CFOUR program [31].

It is known that DFT evaluations of spin–spin coupling constants offer a substantial improvement over HF. However, the stability of spin–spin couplings can be particularly sensitive to the molecular geometries employed [6, 7]. Care must therefore be taken to select appropriate geometries. In Section 4.1, we initially consider 60 isotropic spin–spin couplings for 16 molecules at the CCSD(T)/cc-pVTZ optimized geometries of Refs. [32, 33] to assess the utility of the TDA; for further details of the systems considered, see the supplementary material. Here, we consider all possible couplings, irrespective of isotopic abundance, to maximize the number of data points in assessing the accuracy of the TDA. In Section 4.2, we consider the geometrical dependence of the conventional and TDA spin–spin coupling evaluations in more detail for the CO molecule.

Given the locality of the contributions to the nuclei in Eq. (1), we must take some care when performing practical calculations—in particular, in the choice of basis sets. A range of special basis sets have been developed that augment those used in typical calculations with higher exponent (tight) Gaussian functions. Examples of such sets are the aug-cc-pVXZ-J sets of Sauer *et al.* [34, 35], the augmented sets of Helgaker *et al.* [36], the ccJ-pVNZ sets of Benedikt *et al.* [37], and the pcJ-N basis sets of Jensen [38].

We here utilize the aug-pcJ-*N* series of Jensen [38]. All calculations at DFT, HF and SOPPA(CC) levels are computed using the aug-pcJ-2 basis sets. Preliminary studies showed that the values of isotropic couplings are reasonably well converged at this level. For the CCSD calculations using the CFOUR program, we have used the same basis set where possible, resorting to the aug-pcJ-1 basis sets for some of the larger systems; see the supplementary information for further details [39].

All TDA calculations use an implementation of the response-theory formulation in Section 2.2, which has been tested by also performing selected calculations using the sum-over-states formulation of Section 2.1.

4. Results

Individual values for the calculated indirect nuclear spin–spin couplings can be found in the supplementary information [39].

4.1. *Comparison with Coupled-Cluster Theory*

4.1.1. TDA-HF calculations

We begin by considering the application of the TDA at the HF level of theory. Conventional RHF calculations are exceptionally strongly affected by the triplet instability, with the RHF Coulson–Fischer point (the onset of triplet instabilities) often being close to the equilibrium geometry. This has a strong effect on the the calculated triplet FC and SD components of the spin–spin couplings and, since the FC term often dominates, a seriously detrimental effect on the total spin–spin couplings. Indeed, this effect is often sufficiently severe to render the results practically useless.

In Figure 1, we present a box-whisker plot of the errors for the HF, TDA-HF, SOPPA(CC2) and SOPPA(CCSD) approaches relative to the CCSD data. The HF results shown in the top panel clearly illustrate the issues associated with the conventional evaluation—note the much larger range of errors. The application of the TDA leads to substantial improvement (shown in blue in the lower panel), although a number of significant outliers still remain. The remaining two bars show the comparison of SOPPA(CC2) (orange) and SOPPA(CCSD) (purple) results with the CCSD data. As expected, these values agree reasonably well with the CCSD data except for a few outliers; this comparison indicates that these approaches are of sufficient accuracy to be used as a reference to assess the application of the TDA near to equilibrium molecular geometries.

In Table 1, we present the mean errors and standard deviations (StDev) of the errors for each of the approaches considered in Figure 1. These quantities are shown for the total isotropic spin–spin coupling constant (ISO) as well as for the DSO, PSO, SD and FC components individually. We first note that the DSO contribution is small. Also, the error in this component is unaffected by the response treatment since the component is an expectation value; see Eq. (22).

The PSO term is a singlet contribution; accordingly, the errors in this term at the HF level are modest compared with the errors in the triplet SD and FC terms. Interestingly, the TDA reduces the mean errors and, in particular, the standard deviation in the PSO term further. Whilst, as shown in Section 2.3, the TDA is expected to influence triplet properties most strongly, it affects also singlet properties owing to the reduction of the orbital-rotation Hessian in Eq. (30). The observation that the TDA improves agreement with CCSD results is consistent with recent observations for singlet excited states [13–15].

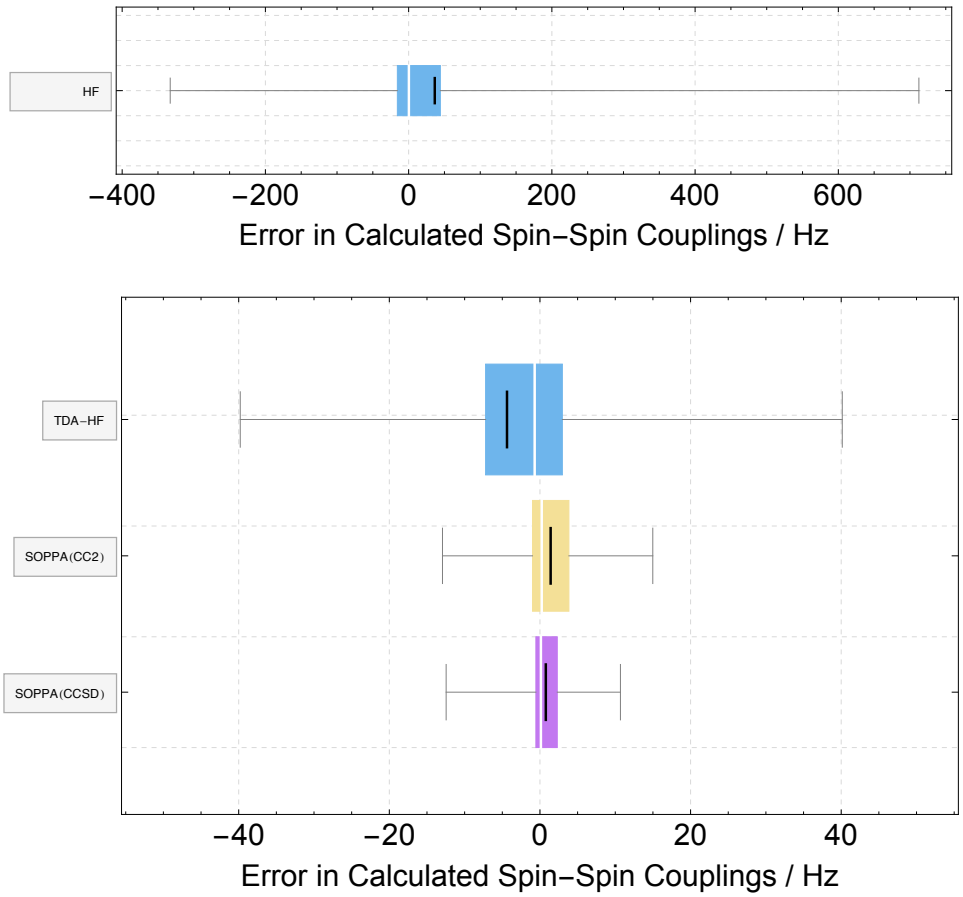

Figure 1. Box-whisker plots of the error in calculated spin–spin coupling constants for HF, TDA-HF, SOPPA(CC2) and SOPPA(CCSD) using the aug-pcJ-2 basis set against CCSD reference data. The left- and right-hand fences of the whiskers denote the maximum negative and positive errors respectively, the white vertical lines denote the median error, the thick black vertical lines denote the mean error, and the left- and right-hand edges of the coloured bar denote the 25% and 75% quantiles respectively.

The triplet-type SD term shows a larger mean error and a very large standard deviation at the HF level. The TDA reduces the error measures substantially, the TDA-HF results being competitive with the SOPPA(CC) approaches, suggesting that the errors in the SD term are dominated by those associated with the triplet instability.

The remaining triplet FC term is often the dominant contribution to the overall isotropic spin–spin coupling constant. Accordingly, this term has the largest mean errors and standard deviations for all approaches. Again, the TDA substantially reduces the error measures. However, in this case, the remaining TDA-HF errors are not competitive with the higher-level methodologies. This behaviour may indicate that the FC errors, although largely arising from the triplet instability, also have a substantial (dynamical) correlation component. For all approaches, the errors in the total isotropic couplings parallel those of the FC term. However, the SOPPA(CC) approaches agree far more closely with the reference coupled-cluster data.

To better examine the range of coupling constants considered here, a correlation plot is presented in Figure 2. The influence of the triplet instability on the HF spin–spin couplings is clear, resulting in almost no correlation with the CCSD results. When the TDA is applied, the improvement is remarkable, all couplings moving much closer to the ideal line. It is notable that, for the larger absolute values of the couplings, the TDA-HF approach produces values systematically below the

Table 1. Mean errors (ME) and standard deviations (StDev) relative to CCSD reference data for the DSO, PSO, SD, FC and total isotropic coupling constants (ISO) using the HF, TDA-HF, SOPPA(CC2) and SOPPA(CCSD) methods with the aug-pcJ-2 basis set.

Method	Error	DSO	PSO	SD	FC	ISO
HF	ME	−0.02	0.06	2.50	33.95	36.49
	StDev	0.03	2.18	32.95	153.00	175.40
TDA-HF	ME	−0.02	−0.17	0.02	−4.21	−4.37
	StDev	0.03	1.12	0.64	13.81	13.58
SOPPA(CC2)	ME	−0.02	0.20	0.05	1.19	1.42
	StDev	0.53	0.92	0.38	5.03	4.78
SOPPA(CCSD)	ME	−0.02	0.20	0.05	0.54	0.78
	StDev	0.53	1.12	0.27	4.12	3.93

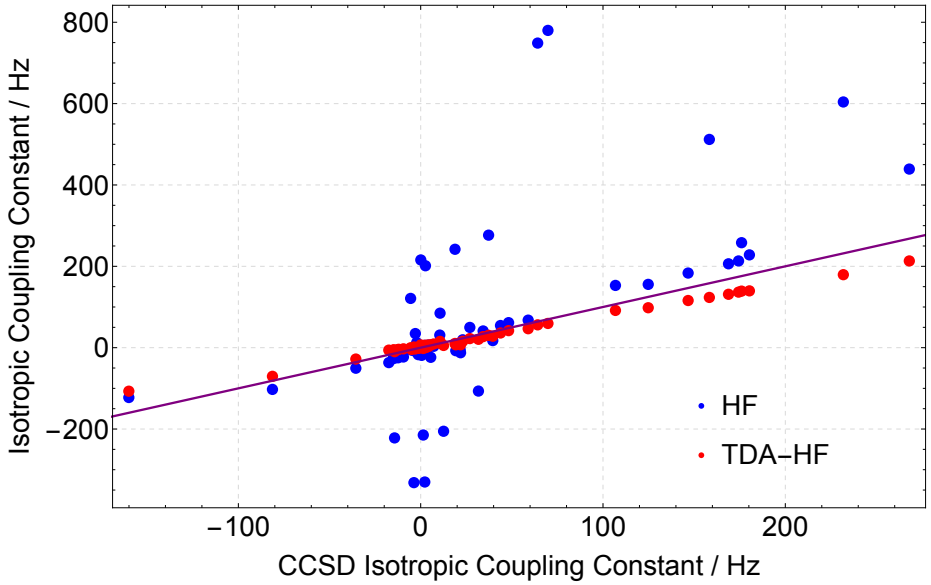

Figure 2. Correlation plot for calculated spin–spin couplings in Hz at the HF (blue points) and TDA-HF (red points) levels with the CCSD couplings. The ideal correlation is shown by the purple line.

corresponding CCSD values.

The improvement in the spin–spin-couplings at the TDA-HF level is encouraging, transforming the results from being of no practical utility into results approaching the quality of conventional KS-DFT. Whilst the results are not of high quality, it should remembered that the cost of TDA-HF calculations is substantially lower than those of SOPPA(CC) and CCSD calculations. Given that the remaining errors at the TDA-HF level result from the neglect of correlation effects, it is interesting to investigate the performance of TDA-DFT methods in this context.

4.1.2. TDA-DFT calculations

To investigate whether TDA-DFT could offer improved accuracy over TDA-HF theory, we performed indirect spin–spin calculations (with and without the TDA) using the following selection of exchange–correlation functionals: LDA [40, 41], BLYP [42, 43], PBE [44], KT2 [45], B3LYP [46, 47], B97-1 [48], B97-2 [49], B97-3 [50], PBE0 [51], and CAM-B3LYP [52]. The quality of the resulting coupling constants is illustrated in Figure 3.

In the upper panel, the results of the conventional coupling evaluations are shown. As might be expected, local-density-approximation (LDA) couplings are of low accuracy. For the generalized-gradient-approximation (GGA) functionals BLYP, KT2, and PBE, we observe a broad range of performance. Interestingly, the KT2

functional, which performs well for the singlet-type shielding constants, does not perform well for the triplet-type spin–spin coupling constants, consistent with previous findings [53]. The PBE results are noticeably more accurate. The hybrid functionals B97-2 and B97-3 stand out as offering the highest accuracy, again consistent with previous work [7, 54]. The range-dependent CAM-B3LYP functional gives results similar to the B3LYP and B97-1 functionals, indicating that the influence of long-range HF exchange on these near-nuclear properties is unimportant.

The lower panel of Figure 3 shows the results upon application of the TDA. Surprisingly, a general deterioration in the quality of the calculated spin–spin coupling constants is evident, as indicated by the width of the coloured bars. Some reduction in the magnitudes of the maximum negative and positive errors is evident however, as shown by the position of the left- and right-hand fences, indicating that some of the most severe outliers are improved by the application of the TDA. However, given the success of the TDA approach in HF theory, the overall deterioration of the results is disappointing. A notable feature of the TDA-DFT results is their uniformity—variations between functionals are greatly reduced. In particular, the quality of the TDA-B97-2/3 results is substantially reduced for most of the couplings. With all exchange–correlation functionals, TDA-DFT tends to underestimate the value of the spin–spin coupling constants.

Table 2 contains the mean errors and standard deviations associated with each exchange–correlation functional, in the same manner as for HF theory in Table 1. As in HF theory, the DSO errors are small. Moreover, the PSO and SD contributions are generally improved by the TDA. For the PSO term, this effect is more pronounced for the hybrid functionals than for the pure functionals. The SD term tends towards underestimating the CCSD value, rather than overestimating it as in the conventional evaluation. Standard deviations are much improved on application of the TDA.

As in HF theory, the FC errors dominate the overall errors in the spin–spin couplings, both with and without the TDA treatment. However, unlike at the HF level, the application of the TDA leads to a general deterioration in the quality of the results, with larger standard deviations and mean errors (with a tendency towards underestimation of the coupling constants). Whilst one might expect an improved FC term due to the potential improvement of triplet excitation energies with the TDA, our results indicate that this is not the case in practice, presumably reflecting the fact that many excitations can contribute and that the numerator in the final term in Eq. (1) is also affected.

Based on the error measures in Table 2, the most accurate TDA-DFT method is TDA-B3LYP. Figure 4 illustrates the correlation of the B3LYP and TDA-B3LYP results with the CCSD values. In the left-hand panel, the full range of couplings is shown. Clearly, the conventional results are not afflicted by the large errors present at the HF level, indicating that the influence of the triplet instability is less severe close to equilibrium geometries for these systems. For larger absolute coupling values, we observe a similar tendency of TDA-B3LYP theory to underestimate the absolute CCSD values as for TDA-HF. In the right-hand panel, we present a more detailed plot for the couplings between -20 and 80 Hz. The TDA-B3LYP results have more scatter than the B3LYP results in this area, leading to poorer error measures consistent with the broadening of the coloured bars in the lower panel of Figure 3.

4.1.3. Comparison of HF and DFT spin–spin coupling constants

A comparison of Tables 1 and 2 shows that, when the TDA is applied, the error measures for the FC contribution become remarkably similar to the HF measures

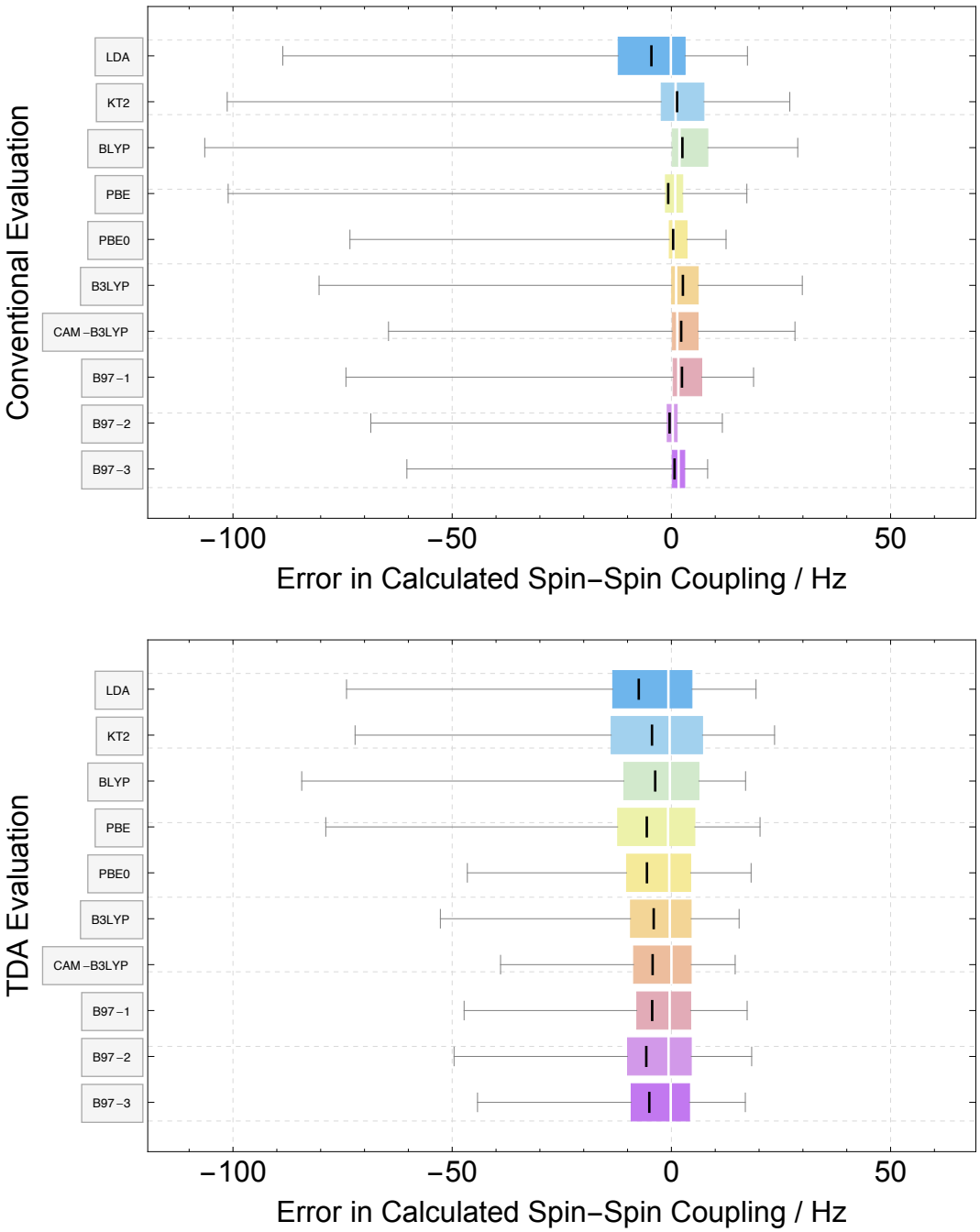

Figure 3. Box-whisker plots of the error in the calculated spin–spin coupling constants for several DFT and TDA-DFT functionals using the aug-pcJ-2 basis set compared against CCSD reference data. The left- and right-hand fences of the whiskers denote the maximum negative and positive errors respectively, the white vertical lines denote the median error, the thick black vertical lines denote the mean error, and the left- and right-hand edges of the coloured bar denote the 25% and 75% quantiles respectively.

for most of the exchange–correlation functionals considered. This observation indicates that, in the calculation of spin–spin coupling constants, standard DFT functionals benefit from a compensation of errors in the treatment of dynamical and static correlation similar to that observed upon bond dissociation.

The application of the TDA removes the negative impact of the triplet instability in the calculation of spin–spin couplings. The fraction of HF exchange present in the density functional does, however, still influence the quality of the KS orbitals

Table 2. Mean errors (ME) and standard deviations (StDev) in the calculated DSO, PSO, SD, FC and total isotropic coupling constants (ISO) for several functionals using DFT and TDA-DFT in the aug-pcJ-2 basis set compared against CCSD reference data.

Method	Error	DSO	PSO	SD	FC	ISO
	Conventional Evaluation					
LDA	ME	0.003	0.28	0.07	−4.91	−4.56
	StDev	0.015	1.13	0.44	16.19	15.54
KT2	ME	−0.011	0.07	0.11	1.13	1.30
	StDev	0.017	0.58	0.77	17.11	16.81
BLYP	ME	−0.004	0.12	0.10	2.30	2.51
	StDev	0.015	0.67	0.61	16.35	16.23
PBE	ME	0.001	0.13	0.10	−0.96	−0.72
	StDev	0.014	0.61	0.57	14.55	14.26
PBE0	ME	−0.005	0.12	0.13	0.15	0.40
	StDev	0.013	0.79	0.86	10.93	10.54
B3LYP	ME	−0.008	0.12	0.11	2.40	2.62
	StDev	0.015	0.82	0.77	13.28	13.03
CAM-B3LYP	ME	−0.010	0.18	0.14	1.92	2.23
	StDev	0.016	1.04	0.98	11.58	10.92
B97-1	ME	−0.005	0.09	0.09	2.24	2.41
	StDev	0.013	0.72	0.48	11.13	11.11
B97-2	ME	−0.006	0.07	0.08	−0.56	−0.41
	StDev	0.014	0.69	0.48	9.38	9.42
B97-3	ME	−0.007	0.10	0.08	0.54	0.71
	StDev	0.014	0.82	0.53	8.53	8.44
	TDA Evaluation					
LDA	ME	0.003	0.03	0.03	−7.50	−7.44
	StDev	0.015	1.07	0.46	20.04	19.62
KT2	ME	−0.011	−0.08	0.01	−4.34	−4.42
	StDev	0.017	0.93	0.36	16.39	16.32
BLYP	ME	−0.004	−0.08	0.02	−3.63	−3.69
	StDev	0.015	0.84	0.36	15.10	15.10
PBE	ME	0.001	−0.08	0.02	−5.55	−5.61
	StDev	0.014	0.86	0.38	17.24	17.15
PBE0	ME	−0.005	−0.08	0.02	−5.52	−5.58
	StDev	0.013	0.76	0.37	15.13	15.02
B3LYP	ME	−0.008	−0.06	0.02	−3.98	−4.04
	StDev	0.015	0.71	0.34	13.10	12.99
CAM-B3LYP	ME	−0.010	−0.01	0.03	−4.30	−4.28
	StDev	0.016	0.79	0.34	13.05	12.79
B97-1	ME	−0.005	−0.09	0.01	−4.29	−4.38
	StDev	0.013	0.76	0.43	13.79	13.74
B97-2	ME	−0.006	−0.11	0.00	−5.62	−5.73
	StDev	0.014	0.79	0.45	15.58	15.57
B97-3	ME	−0.007	−0.09	0.01	−4.95	−5.04
	StDev	0.014	0.74	0.43	14.27	14.21

and eigenvalues obtained and so the final value of the isotropic coupling constant. To investigate this effect, we considered a range of hybrid functionals based on the PBE functional of the form

$$E_{\mathrm{xc}}^{\mathrm{PBEh}} = a_x E_{\mathrm{x}}^{\mathrm{HF}} + (1 - a_x) E_{\mathrm{x}}^{\mathrm{PBE}} + E_{\mathrm{c}}^{\mathrm{PBE}}. \tag{31}$$

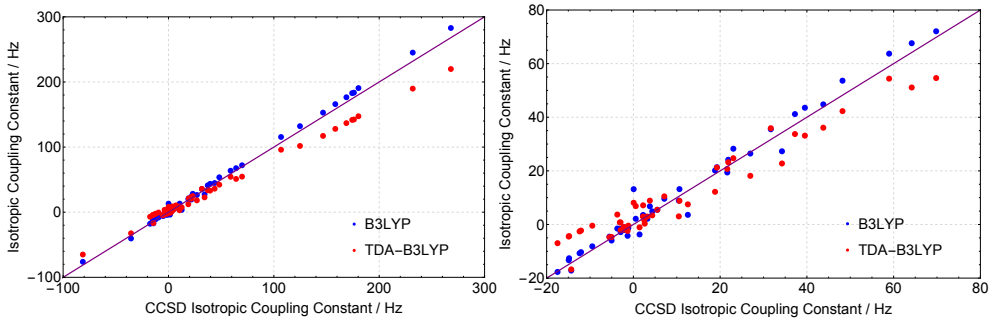

Figure 4. Correlation plot for calculated spin–spin couplings in Hz at the B3LYP (blue points) and TDA-B3LYP (red points) levels with the CCSD couplings. The ideal correlation is shown by the orange line.

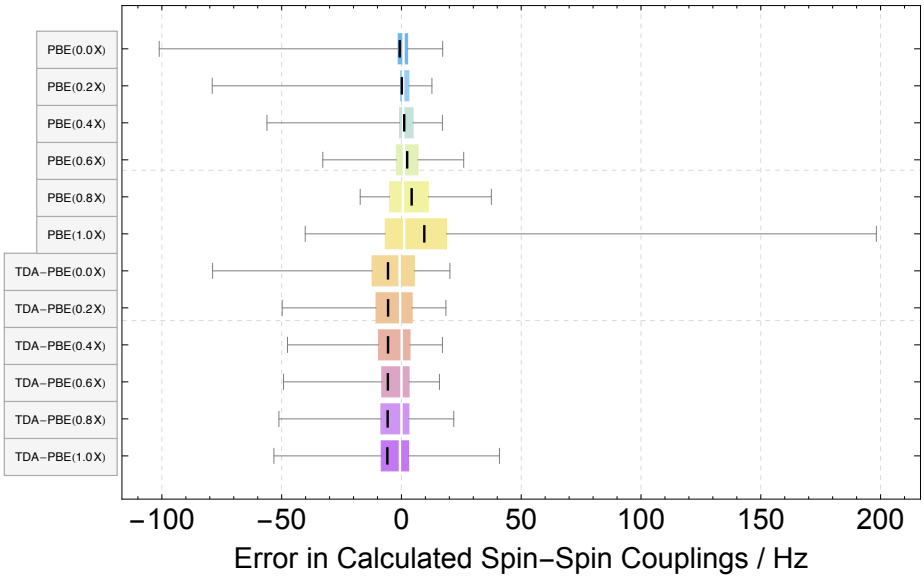

Figure 5. DFT and TDA-DFT errors in calculated spin–spin coupling constants for the PBE functional with various amounts of HF exchange using the aug-pcJ-2 basis compared with CCSD reference data.

The results for a series of functionals with $a_x = 0.0, 0.2, 0.4, 0.6, 0.8, 1.0$ are shown in Figure 5.

Comparing the top and bottom panels, we see that, whereas the DFT results obtained conventionally deteriorate for the bulk of the couplings (as expected) as more HF exchange is introduced, the variation with the fraction HF exchange is much less pronounced when the TDA is applied. This behaviour again hints towards error cancellations between the treatment of static and dynamical correlation by density-functional approximations.

4.2. *Geometry Dependence of the Spin–Spin Coupling Constant in CO*

So far, the analysis has focussed on nuclear spin–spin couplings evaluated close to molecular equilibrium geometries. However, it is well known that the evaluation of spin–spin couplings is very sensitive to the choice of molecular geometry. In particular, Lutnæs *et al.* [7] showed that some of the more accurate functionals such as B97-2/3 are particularly sensitive to the choice of geometry, whilst less accurate forms such as LDA are more robust. This geometrical stability correlates with the extent to which the methods are influenced by triplet instabilities close to the equilibrium geometry.

To investigate this issue further, we considered the variation of the coupling

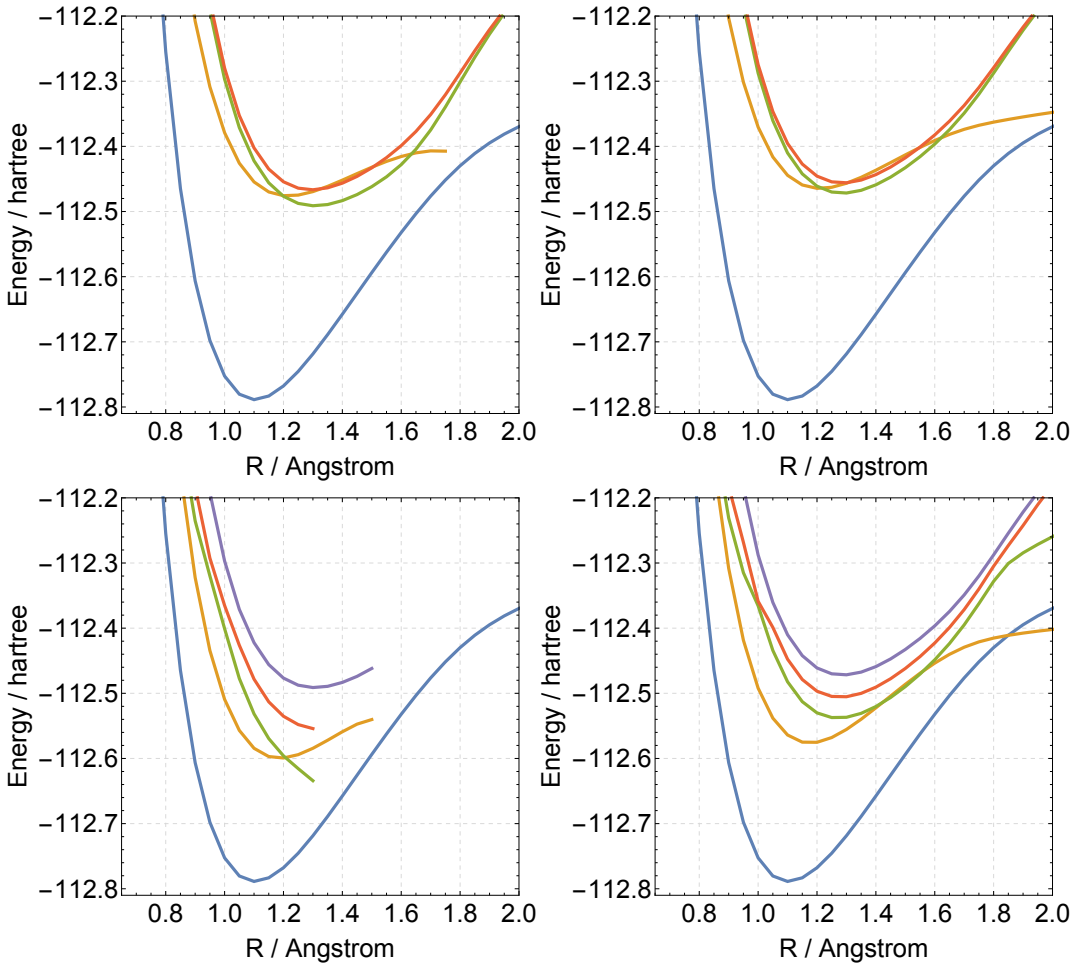

Figure 6. The lowest singlet (top) and triplet (bottom) excited states of the CO molecule calculated using TD-HF (left) and TDA-TD-HF (right) linear response theory. The energies are given in hartree and the bond lengths in Å.

constants as a function of bond length for all of the diatomics in our dataset. In all cases, we found a similar behaviour. We therefore discuss here only the behaviour of the spin–spin coupling constant in the CO molecule.

4.2.1. HF and TDA-HF spin–spin coupling constant of CO

In Figure 6, we have plotted HF energy curves of CO calculated using response theory. The top panels contain the dissociation curves of the ground state and the three lowest singlet excited states, calculated in the conventional HF manner (left) and using the TDA (right). The bottom panels contain the corresponding curves for the ground state and four lowest triplet states.

As expected, the TDA has little effect on the singlet excitation energies, influencing only the lowest excitation energy at 1.8 Å significantly. By contrast, it has a large influence on triplet excitation energies. In particular, the lowest three excited states without the TDA can only be calculated up to approximately 1.4 Å; beyond this distance the excitation energies become imaginary. Even before this point, the calculated states show unphysical behaviour.

When the TDA is applied, all states show a more physical behaviour and can be calculated out to arbitrary internuclear separation. This behaviour is consistent with the fact that the TDA is equivalent to the configuration-interaction-singles (CIS) approximation, the variational nature this approach imparting stability to the TDA excited states.

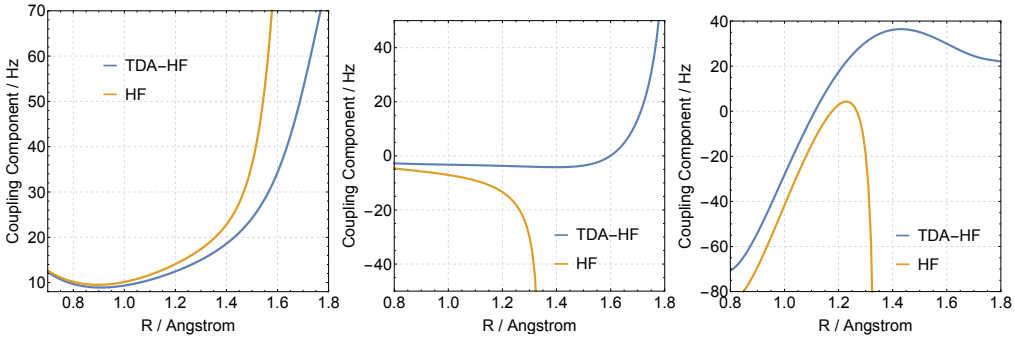

Figure 7. The PSO, SD and FC components of the spin–spin coupling constant (Hz) in CO molecule as a function of bond length (Å), calculated at the HF (orange) and TDA-HF (blue) levels.

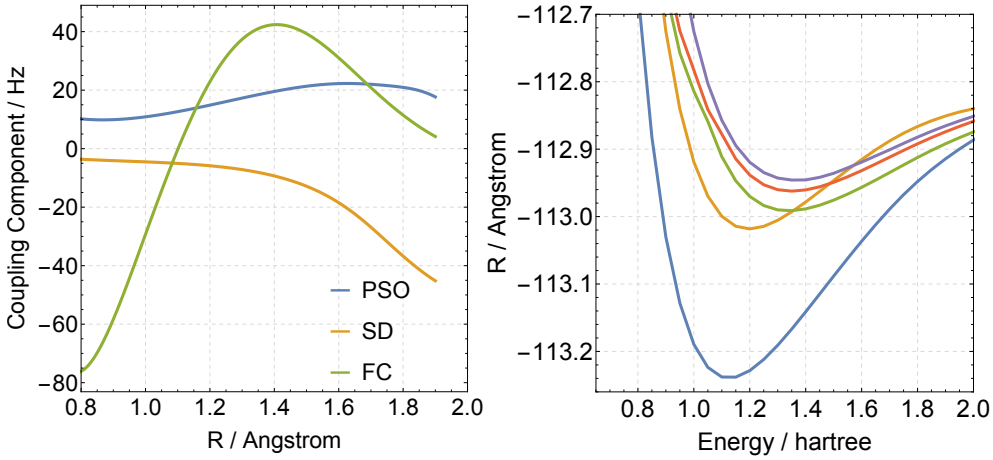

Figure 8. CCSD spin–spin coupling components (Hz) and triplet excited state energies as a function of bond length (Å).

In Figure 7, we present the components of the spin–spin coupling constant in CO as a function of bond length. The DSO term is not shown since it is not affected by the application of the TDA and it gives a small contribution in comparison to the other components. The increase in the PSO term with increasing bond length is slightly less with the application of the TDA.

As expected from the energy curves in Figure 6, we see much stronger geometry effects in the SD and FC terms. In both cases, the HF coupling constant tends towards large negative values between 1.2 and 1.4 Å, consistent with the bond lengths at which the triplet excitation energies become unreliable. The application of the TDA (blue curves) leads to more reasonable SD and FC values for a much broader range of bond lengths.

It is noteworthy that the SD term shows a sharp upturn around 1.6 Å, as does the PSO term. At this geometry, the RHF ground state itself is becoming unreliable, approaching the excited state singlet curves and (in the TDA case) crossing the lowest triplet curves. Whilst the TDA can help to remove the influence of the triplet instability in the calculation of excitation energies, the remaining reduced orbital-rotation Hessian ${}^{u}\mathbf{A}$ is still dependent on the quality of the the ground state orbitals and eigenvalues and so we may not expect accurate results at very stretched geometries.

For comparison, we have plotted the corresponding CCSD spin–spin coupling constant components and triplet excited-state curves of CO in Figure 8. Qualitatively, the CCSD energy curves are are much more similar to the TDA-HF curves than to the HF curves until about 1.5 Å, where the RHF reference state starts to become insufficiently accurate.

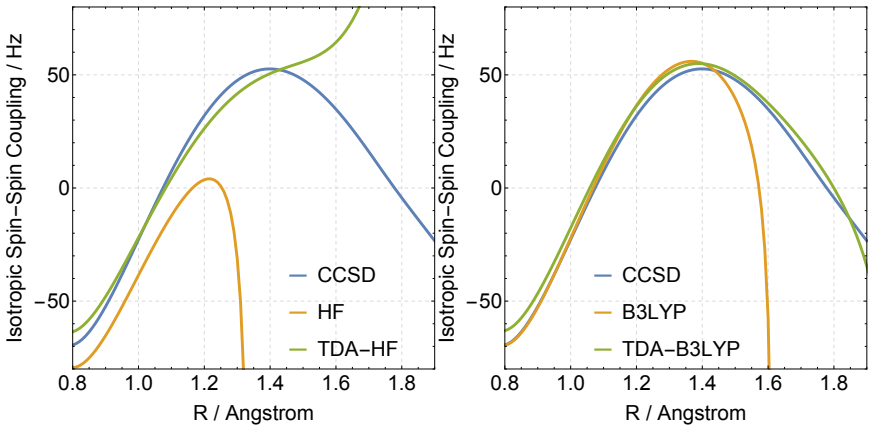

Figure 9. Comparison of HF / TDA-HF and DFT / TDA-DFT results with CCSD total isotropic coupling constants (Hz) as a function of bond length (Å).

Finally, we have in the left-hand panel of Figure 9 plotted the geometry dependence of the total spin–spin coupling constant of CO at the HF, TDA-HF and CCSD levels of theory. The dramatic improvements from HF to HF-TDA theory is clearly illustrated—in fact, the HF-TDA coupling constant is quite similar to the CCSD constant up to a bond length of about 1.4 Å.

4.2.2. B3LYP and TDA-B3LYP spin–spin coupling constant of CO

Qualitatively, the B3LYP and TDA-B3LYP energy curves depicted in Figure 10 resemble those for HF and TDA-HF in Figure 6. However, there are a couple of important differences. Firstly, the onset of issues associated with the triplet instability is much later for the B3LYP triplet states—namely, beyond 1.5 Å, compared with 1.2 Å at the HF level. Secondly, the B3LYP ground-state energy curve is reasonable for a wider range of internuclear separations. In particular, at stretched geometries, the energy curve rises less quickly and so crossings occur at longer bond lengths when the TDA is applied.

The geometry dependence of the components of the B3LYP and TDA-B3LYP spin–spin couplings reflect these observations, see Figure 11, to be compared with Figure 7 for HF theory. In particular, the later onset of triplet instability issues is reflected in the much improved agreement between the conventional and TDA SD and FC components for a much broader range of bond lengths than in Figure 7. The more reasonable B3LYP ground-state energy curve close to equilibrium is reflected in the substantially different behaviour of the PSO term compared with Figure 7.

In the right-hand panel of Figure 9, the comparison of the overall isotropic spin–spin coupling constant with CCSD as a function of the internuclear separation is presented. The behaviour at bond lengths up to 1.4 Å is similar, whether or not the TDA is applied. In fact, a slight reduction in accuracy is observed near equilibrium when the TDA is applied, in agreement with the observations of Section 4.1 for the full set of molecules. However, for bond lengths between 1.4 and 1.8 Å, the TDA offers a significant improvement, agreeing well with the CCSD reference curve. In the context of DFT, the main result of the application of the TDA is a more global stability of the spin–spin couplings as a function of geometry. However, expectations of this stability must be tempered by the realization that the TDA cannot correct deficiencies in the reference state.

4.2.3. Variation with exchange–correlation functional

Finally, we consider how the geometry dependence of the spin–spin coupling constant in CO is affected by the choice of density-functional approximation. As a representative selection, we present results for LDA, PBE and B3LYP in Figure 12.

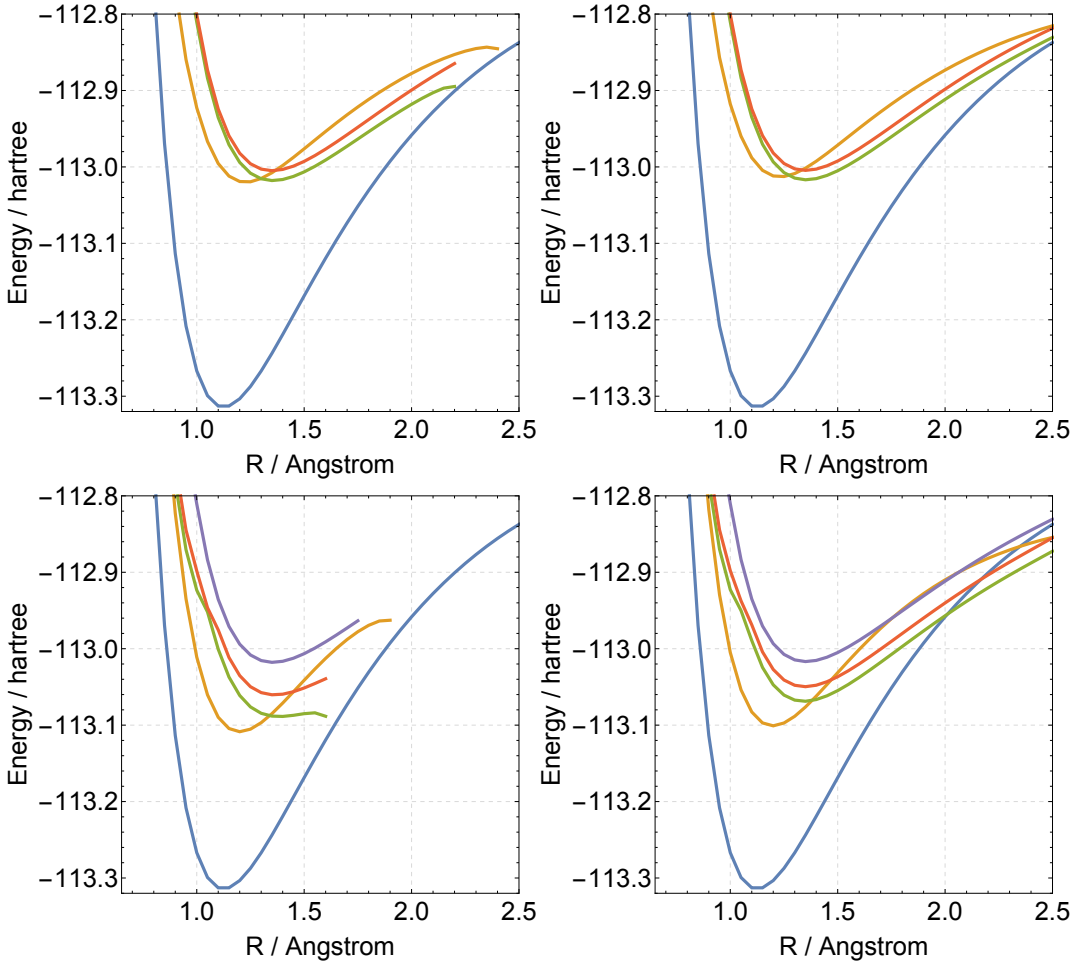

Figure 10. The ground state and three lowest singlet (top) and triplet (bottom) excited states of the CO molecule calculated using TD-DFT (left) and TDA-TD-DFT (right) linear response theory with the B3LYP functional. The energies are given in hartree and the bond lengths in Å.

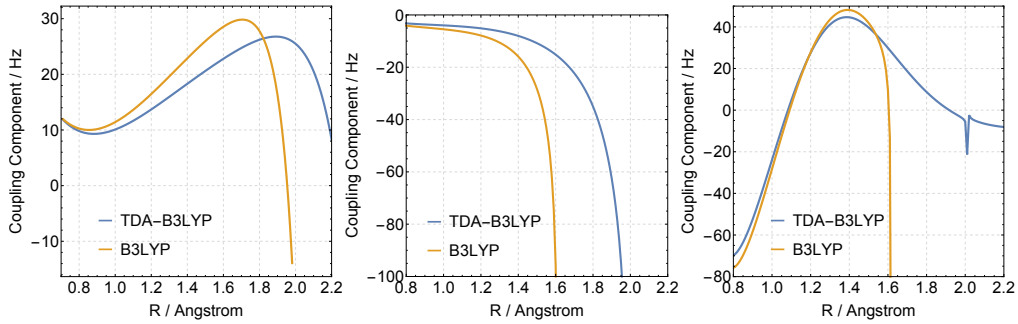

Figure 11. The PSO, SD and FC components of the spin–spin coupling constant (Hz) in CO molecule as a function of bond length (Å), calculated at the B3LYP (orange) and TDA-B3LYP (blue) levels.

Without the TDA, we see that the breakdown of the isotropic spin–spin coupling constants as the bond length increases occurs first for B3LYP, then PBE and finally for LDA, consistent with the observations of Lutnæs *et al.* [7]. Remarkably, when the TDA is applied, all three functionals give very similar results for bond lengths up to 1.8 Å. This result is consistent with those in the previous section, suggesting that, to some extent at least, the accuracy of some functionals in the conventional evaluation of spin–spin coupling constants may be dependent on error cancellation.

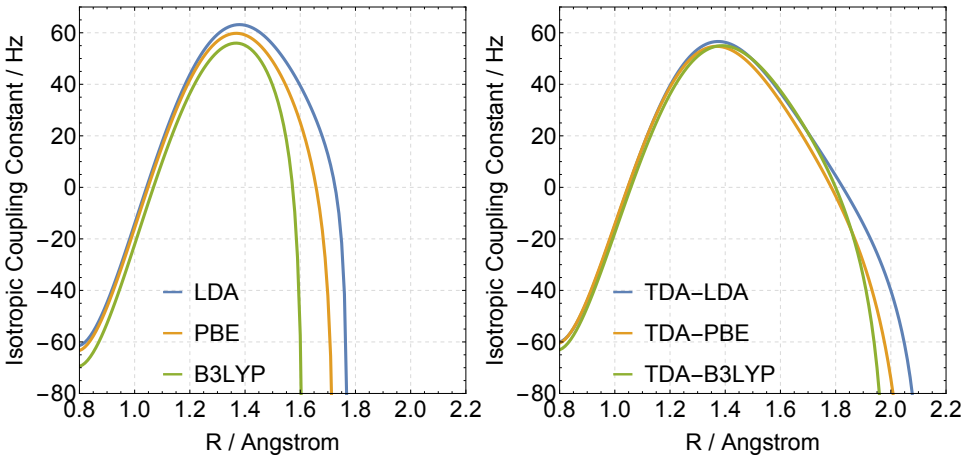

Figure 12. Isotropic spin–spin coupling constants as a function of internuclear separation calculated using a variety of density-functional approximations in the conventional manner and with the application of the TDA.

5. Conclusions

The application of the TDA to the calculation of indirect nuclear spin–spin coupling constants has been explored. The calculation of these constants is particularly challenging since they are composed of several contributions of quite different character. The DSO contribution is a simple ground-state expectation value, the PSO contribution requires an accurate treatment of singlet excited states, and the SD and FC contributions require an accurate treatment of triplet excited states.

At the HF level of theory, the errors due to triplet instabilities are dominant, making the application of the TDA remarkably effective. In fact, practically meaningless results are transformed into results of semi-quantitative accuracy. Furthermore, the TDA-HF results show stability over a reasonably wide range of geometries.

For the density-functional approximations, the application of the TDA at the equilibrium geometry led to a slight decrease in accuracy. Nevertheless, the TDA results are more reliable over a broader range of bond lengths, making it less important to have optimized geometries available at a given level of theory to perform spin–spin coupling calculations. A notable feature of the TDA-DFT results is their uniformity—indicating the possibility that existing functionals exhibiting reasonable accuracy trade-off between errors in the dynamical and static correlation energies.

An important message from this study is that, to achieve high accuracy, it is necessary for the reference state to be of reasonable accuracy. The TDA can overcome issues associated with the triplet instability in the determination of response quantities—however, if the orbitals and eigenvalues entering the reduced orbital-rotation Hessian ${}^{u}\mathbf{A}$ are not sufficiently accurate, such as at very stretched geometries, then high accuracy cannot be expected. This essentially determines the 'window of opportunity' in which simple approximations like the TDA may have a positive effect. The uniformity of the TDA-DFT results may suggest that, for further progress in the calculation of spin–spin couplings at the DFT level, it is essential to improve the description of electronic correlation effects in both ground and excited states.

6. Acknowledgements

Nick Handy was an inspiring and enthusiastic teacher, supervisor and researcher, and he was also a great friend. It was a pleasure to know him and to work with him.

A. M. T. is grateful for support from the Royal Society University Research Fellowship scheme. M. S. R. is grateful to the University of Nottingham and the Royal Society for summer studentship support as part of this work. We are grateful for access to the University of Nottingham High Performance Computing Facility. This work was supported by the Norwegian Research Council through the CoE Centre for Theoretical and Computational Chemistry (CTCC) Grant No. 179568/V30 and the Grant No. 171185/V30 and through the European Research Council under the European Union Seventh Framework Program through the Advanced Grant ABACUS, ERC Grant Agreement No. 267683. D. J. T. and M. J. G. P. are grateful to the EPSRC for financial support.

References

[1] J. Čižek and J. Paldus, *J. Chem. Phys.* **47**, 3976 (1967)
[2] R. Seeger and J.A. Pople, *J. Chem. Phys.* **66**, 3045 (1977)
[3] R. McWeeny, *Methods of Molecular Quantum Mechanics*, 2nd ed. (Academic Press, London, 1992)
[4] P. Jørgensen and J. Simons, *Second Quantization-Based Methods in Quantum Chemistry.* (Academic Press, New York, 1981)
[5] R. Bauernschmitt and R. Ahlrichs, *J. Chem. Phys.* **104**, 9047 (1996)
[6] T. Helgaker, O.B. Lutnæs and M. Jaszuński, *J. Chem. Theory Comput.* **3**, 86 (2007)
[7] O. B. Lutnæs, T. Helgaker and M. Jaszuński, *Mol. Phys.* **108**, 2579 (2010)
[8] I. Tamm *J. Phys. USSR* **9**, 449 (1945)
[9] S. M. Dancoff *Phys. Rev.* **78**, 382 (1950)
[10] R. Bauernschmitt and R. Ahlrichs, *Chem. Phys. Lett.***256**, 454 (1996)
[11] S. Hirata and M. Head-Gordon, *Chem. Phys. Lett.* **314**, 291 (1999)
[12] C. Jamorski, M. E. Casida, and D. R. Salahub, *J. Chem. Phys.* 104 5134 (1996)
[13] M. J. G. Peach , M. J. Williamson, and D. J. Tozer, *J. Chem. Theory Comput.* **7** 3578 (2011)
[14] M. J. G. Peach and D. J. Tozer, *J. Phys. Chem. A* **116** 9783 (2012)
[15] M. J. G. Peach, N. Warner, and D. J. Tozer, *Mol. Phys.* **111** 1271 (2013)
[16] J. S. Sears, T. Koerzdoerfer, C.-R. Zhang, and J.-L. Bredas, *J. Chem. Phys.* **135** 151103 (2011)
[17] T. Helgaker and M. Pecul, in *Calculation of NMR and EPR Parameters: Theory and Applications*, M. Kaupp, M. Bühl, and V. G. Malkin, eds. (Wiley-VCH, Weinheim 2004), pp. 101–121
[18] N. F. Ramsey, *Phys. Rev.* **91**, 303 (1953)
[19] H. Fukui, *Prog. NMR Spec.* **35**, 267 (1999)
[20] M. F. Guest, V. R. Saunders, R. E. Overill, *Mol. Phys.* **35**, 427 (1978)
[21] J. Olsen, D. L. Yeager, and P. Jørgensen, *J. Chem. Phys.* **91**, 381, (1989)
[22] O. Vahtras, H. Ågren, P. Jørgensen, H. J. Aa. Jensen, T. Helgaker, and J. Olsen, *J. Chem. Phys.* **97**, 9178, (1992)
[23] P. Jørgensen, H. J. Aa. Jensen, and J. Olsen, *J. Chem. Phys.* **89**, 3654, (1988)
[24] DALTON, a molecular electronic structure program, Release Dalton2013 (2013), see http://daltonprogram.org/
[25] K. Aidas, C. Angeli, K. L. Bak, V. Bakken, R. Bast, L. Boman, O. Christiansen, R. Cimiraglia, S. Coriani, P. Dahle, E. K. Dalskov, U. Ekström, T. Enevoldsen, J. J. Eriksen, P. Ettenhuber, B. Fernández, L. Ferrighi, H. Fliegl, L. Frediani, K. Hald, A. Halkier, C. Hättig, H. Heiberg, T. Helgaker, A. C. Hennum, H. Hettema, E. Hjerteniæs, S. Høst, I.-M. Høyvik, M. F. Iozzi, B. Jansík, H. J. Å. Jensen, D. Jonsson, P. Jørgensen, J. Kauczor, S. Kirpekar, T. Kjærgaard, W. Klopper, S. Knecht, R. Kobayashi, H. Koch, J. Kongsted, A. Krapp, K. Kristensen, A. Ligabue, O. B. Lutnæs, J. I. Melo, K. V. Mikkelsen, R. H. Myhre, C. Neiss, C. B. Nielsen, P. Norman, J. Olsen, J. M. H. Olsen, A. Osted, M. J. Packer, F. Pawlowski, T. B. Pedersen, P. F. Provasi, S. Reine, Z. Rinkevicius, T. A. Ruden, K. Ruud, V. Rybkin, P. Sałek, C. C. M.

Samson, A. Sánchez de Merás, T. Saue, S. P. A. Sauer, B. Schimmelpfennig, K. Sneskov, A. H. Steindal, K. O. Sylvester-Hvid, P. R. Taylor, A. M. Teale, E. I. Tellgren, D. P. Tew, A. J. Thorvaldsen, L. Thøgersen, O. Vahtras, M. A. Watson, D. J. D. Wilson, M. Ziolkowski and H. Åagren, "The Dalton quantum chemistry program system" *WIRES Comput. Mol. Sci.* **4** (2014), doi:10.1002/wcms.1172

[26] J. Oddershede, P. Jørgensen and D. Yeager, *Comput. Phys. Rep.* **2**, 33, (1984)

[27] S. P. A. Sauer, *J. Phys. B: At. Mol. Phys.* **30**, 3773, (1997)

[28] H. Kjær, S. P. A. Sauer, and J. Kongsted. *J. Chem. Phys.* **133**, 144106, (2010)

[29] T. Enevoldsen, J. Oddershede, and S. P. A. Sauer. *Theor. Chem. Acc.*, **100**, 275, (1998)

[30] A.A. Auer and J. Gauss, *Chem. Phys.* **356**, 7 (2001)

[31] CFOUR, a quantum chemical program package written by J.F. Stanton, J. Gauss, M.E. Harding, P.G. Szalay with contributions from A.A. Auer, R.J. Bartlett, U. Benedikt, C. Berger, D.E. Bernholdt, Y.J. Bomble, O. Christiansen, M. Heckert, O. Heun, C. Huber, T.-C. Jagau, D. Jonsson, J. Jusélius, K. Klein, W.J. Lauderdale, D.A. Matthews, T. Metzroth, D.P. O'Neill, D.R. Price, E. Prochnow, K. Ruud, F. Schiffmann, S. Stopkowicz, A. Tajti, J. Vázquez, F. Wang, J.D. Watts and the integral packages MOLECULE (J. Almlöf and P.R. Taylor), PROPS (P.R. Taylor), ABACUS (T. Helgaker, H.J. Aa. Jensen, P. Jørgensen, and J. Olsen), and ECP routines by A. V. Mitin and C. van Wüllen. For the current version, see http://www.cfour.de.

[32] O. B. Lutnæs, A. M. Teale, T. Helgaker, D. J. Tozer, K. Ruud and J. Gauss, *J. Chem. Phys.* **131**, 144104 (2009)

[33] A. M. Teale, O. B. Lutnæs, T. Helgaker, D. J. Tozer and J. Gauss, *J. Chem. Phys.* **138**, 024111 (2013)

[34] T. Enevoldsen, J. Oddershede and S. P. A. Sauer, *Theor. Chem. Acc.* **100**, 275 (1998)

[35] P. F. Provasi, G. A. Aucar and S. P. A. Sauer, *J. Chem. Phys.* **115**, 1324 (2001)

[36] T. Helgaker, M. Jaszuński, K. Ruud and A. Górska, *Theor. Chem. Acc.* **99**, 175 (1998)

[37] U. Benedikt, A. A. Auer, F. Jensen, *J. Chem. Phys.* **129**, 064111 (2008)

[38] F. Jensen *J.* Chem. Theory Comput. **2**, 1360 (2006)

[39] The Supplementary Information

[40] P. Hohenberg and W. Kohn, Phys. Rev. **B**. **136**, B864 (1964).

[41] S. J. Vosko, L. Wilk and M. Nusair, Can. J. Phys. **58**, 1200 (1980).

[42] A. D. Becke, Phys. Rev. **A**. **38**, 3098 (1988).

[43] C. Lee, W. Yang and R. G. Parr, Phys. Rev. **B**. **37**, 785 (1988).

[44] J. P. Perdew, K. Burke and M. Ernzerhof, Phys. Rev. Lett. **77**, 3865 (1996).

[45] T. W. Keal and D. J. Tozer, J. Chem. Phys. **119**, 3015 (2003).

[46] P. J. Stephens, F. J. Devlin, C. F. Chabalowski and M. J. Frisch, J. Phys. Chem. **98**, 11623 (1994).

[47] A. D. Becke, *J. Chem. Phys.* **98**, 5648 (1993).

[48] F. A. Hamprecht, A. J. Cohen, D. J. Tozer and N. C. Handy, *J. Chem. Phys.* **109**, 6264 (1998).

[49] P. J. Wilson, T. J. Bradley and D. J. Tozer, *J. Chem. Phys.* **115**, 9233 (2001).

[50] T. W. Keal and D. J. Tozer, *J. Chem. Phys.* **123**, 121103 (2005).

[51] C. Adamo and V. Barone, *J. Chem. Phys.* **110**, 6158 (1999).

[52] T. Yanai, D. P. Tew and N. C. Handy, *Chem. Phys. Lett.* **393**, 51 (2004).

[53] T. W. Keal, D. J. Tozer, and T. Helgaker, *Chem. Phys. Lett.* 391, 374 (2004)

[54] T. W. Keal, T. Helgaker, P. Salek, and D. J. Tozer, *Chem. Phys. Lett.* 425, 163 (2006)